ELSEVIER

Catalysis Today 61 (2000) 137–141

CATALYSIS TODAY

www.elsevier.com/locate/cattod

Catalytic hydroxylation of benzene over vanadium-containing molecular sieves

Chul Wee Lee, Woo Jin Lee, Yong Ki Park, Sang-Eon Park*

Industrial Catalysis Research Laboratory, Korea Research Institute of Chemical Technology (KRICT),
PO Box 107, Yusung, Taejon 305-606, South Korea

Abstract

Vanadium-containing molecular sieves with mesopore structures such as MCM-41 and MCM-48, and micropore structures such as BEA and MFI were synthesized by hydrothermal method. XRD, FT-IR, UV–Vis DRS, EPR and XANES were used to characterize their structure, electronic states, and active sites of vanadium species. All the vanadium containing molecular sieves exhibit a pre-edge peak in the V K-edge XANES. The charge transfer transition bands appear at 250 and 340 nm are attributed to the $[V^V{=}O]^{3+}$ species in the tetrahedral framework position and in the surface wall, respectively. Upon calcining the as-synthesized vanadium-containing samples in the air, V^{IV} species are oxidized to V^V which is EPR silent. V^V is reduced reversibly by dehydration at 723 K. As for catalytic hydroxylation of benzene, V-MCM-41 shows the highest activity where the turnover number is 64 h^{-1} at 343 K. Under the higher temperature and the higher acidic conditions, respectively, the catalytic activity is enhanced. © 2000 Elsevier Science B.V. All rights reserved.

Keywords: Hydroxylation of benzene; Vanadium-containing molecular sieves; UV–Vis DRS; XANES; EPR; FT-IR

1. Introduction

Recently much interest is focused on the synthesis and application of transition metal incorporated mesoporous materials such as MCM-41 and MCM-48 [1] as well as microporous molecular sieves. Various transition metals such as Ti [2], V [3], Fe [4], Mn [5], and Cr [6] containing molecular sieves having redox catalytic properties have been synthesized by hydrothermal method. Also these materials show high catalytic activities for the oxidation of organic compounds such as benzene [2], phenol [7] or cyclohexene [8] by H_2O_2. It is not easy to get the relatively higher conversion of benzene oxidation due to the difficulty of overcoming its resonance energy. To understand the mechanism of hydroxylation of aromatic compounds over the vanadium sites in the molecular sieves, various kinds of studies have been attempted. Sivasanker and coworkers [9] have suggested that tetrahedral vanadium species (V^{5+}) having redox properties in the framework of ZSM-11 system is the only active site for oxidation of phenol [9]. On the other hand, some researchers have suggested the possibility of formation of phenol from hydroxylation of benzene by in situ generation of H_2O_2 over Pd-containing silica or Pd/TS-1 [10,11], where Pd is used for activating the H_2 molecule to produce H_2O_2. Vanadium-containing mesoporous materials such as V-MCM-41 showed good catalytic activity for the oxidation of benzene over bicatalytic system with Pd-metal catalysts in our previous work [12]. In this work, we have synthesized and characterized various

---

* Corresponding author. Tel.: +82-42-860-7670;
fax: +82-42-860-7676.
E-mail address: separk@pado.krict.re.kr (S.-E. Park).

PII: S0920-5861(00)00357-6

V-containing molecular sieves, and investigated their catalytic activity for benzene hydroxylation.

2. Experimental

2.1. Synthesis

According to the literatures, V-containing molecular sieves of mesopore structures such as MCM-41 [3] and MCM-48 [13], and micropore structures such as BEA [14] and MFI [15] were synthesized by hydrothermal method. The hydrothermal synthesis of vanadium-containing molecular sieves was carried out with the following molar composition for each structure. SiO_2:0.018 VO_2:0.17 Na_2O:0.5 RBr:30 H_2O for V-MCM-41, SiO_2:0.01 VO_2:0.25 NaO_2:0.64 RCl:62 H_2O for V-MCM-48, SiO_2:0.017 V_2O_5:0.5 TEAOH:26 H_2O:7.3 H_2O_2 for V-BEA, and SiO_2:0.02 $VOSO_4$:0.11 NH_3:0.11 TPAOH:12 H_2O for VS-1, RCl and RBr designated as the organic surfactant. In a typical synthesis, tetraethylorthosilicate (Aldrich) was dissolved in a NaOH solution or an aqueous NH_3 solution and stirred for 15–30 min. Then a vanadium precursor such as $VOSO_4$ or V_2O_5 (Aldrich) was added to the mixture dropwise with vigorous stirring, and stirred for 1 h before adding the templates such as TPAOH or TEAOH for BEA-structure and MFI-structure, respectively, or surfactant such as cetyltrimethylammonium chloride or bromide as an organic surfactant for MCM-41 and MCM-48, respectively. After stirring for three additional hours, the final gel mixture was transferred to a Teflon lined stainless-steel autoclave and kept at 383 K for V-MCM-41 and V-MCM-48, respectively, and at 413 or 443 K for V-BEA and VS-1, respectively. But crystallization times are various such as 3 days for V-MCM-48, 6 days for V-MCM-41, 20 days for V-BEA, and 4 days for VS-1, respectively. The final as-synthesized product was filtered, washed with hot distilled water and dried at 353 K for 12 h. Surfactant and template were removed by calcining in the air at 823 K for 6 h.

2.2. Characterization

X-ray powder diffraction (Rigaku, 2155D6) was employed to investigate the structure of molecular sieves over the range $1.5^\circ < 2\Theta < 10^\circ$ for mesoporous materials and $1.5^\circ < 2\Theta < 60^\circ$ for microporous materials. UV–Vis DRS was measured with a Shimadzu UV-2501PC spectrophotometer equipped with a reflectance attachment and $BaSO_4$ was used as the reference material. EPR spectra were collected at 77 K with a Bruker ESR spectrometer (Model ESP 300) and the microwave frequency was measured by Hewlett-Packard frequency counter (Model HP5350B).

2.3. Catalytic activity measurements

Catalyst (0.05–0.2 g), 6 ml of benzene (Aldrich, anhydrous), and 6 ml of concentrated acetic acid were placed in the flask equipped with condenser connecting to chiller, and stirred with a magnetic stirrer. H_2O_2 (30% solution, Fluka) was added to the flask dropwise by syringe pump at a rate of 2.5 ml/h. After reaction, the organic and aqueous resultant solutions were analyzed, respectively, by GC at 523 K (Chrompack; CP-SIL 5CB 25 m capillary column).

3. Results and discussion

3.1. Spectroscopic characterization

XRD patterns for V-containing molecular sieves prepared in this work is identical to their vanadium-free analogues such as H-BEA, silicalite-1, MCM-41, and MCM-48. XRD results of all vanadium-containing materials are well structured without any vanadyl clusters.

UV–Vis DRS of V-incorporated molecular sieves before and after dehydration are shown in Fig. 1, and their band assignments are summarized in Table 1. All calcined/dehydrated V-containing samples show strong UV–Vis absorption bands around 220 and 250 nm, and a broad shoulder at 340 nm due to the charge transfer (CT) transition between metal and ligand. Experimentally, all molecular sieves prepared in this study without vanadium show UV–Vis band at 220 nm, which might be due to silica in the molecular sieves. The CT bands are strongly influenced by the local structure of vanadium sites and also isolated vanadium species generally give rise to CT transitions in a higher energy region than polymeric species. The

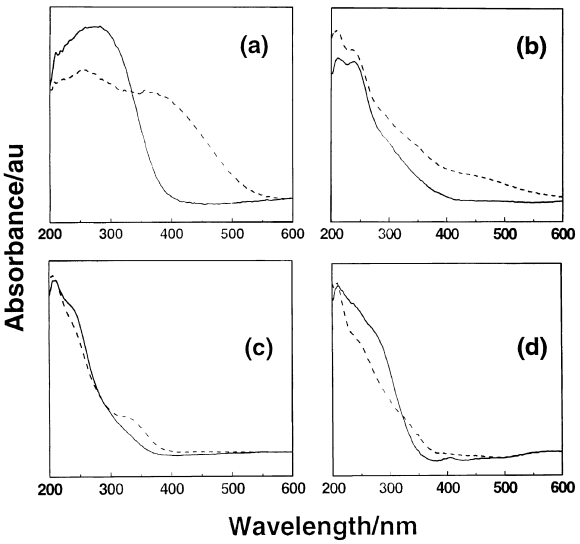

Fig. 1. UV–Vis DRS of: (a) V-MCM-41, (b) V-MCM-48, (c) VS-1, and (d) V-BEA, hydrated (dashed lines) and dehydrated (solid lines) samples.

absorption band in the region of 333–500 nm is associated with the lower-energy charge transfer (LCT) of O–V^{5+} electron transfer for octahedral coordination [16]. In the case of V^{4+}, the LCT transition is expected to show at a higher wavelength of 250–285 nm [9,18]. Kornatowski et al. [19] have suggested that two bands at ca. 295 and 340 nm correspond to the LCT assigned to O–V electron transfer $(\pi)t_2 \rightarrow (d)e$ and $(\pi)t_1 \rightarrow (d)e$, respectively, in the V-silicalite samples. Kevan and coworkers [16] have reported that the band at 275 nm is attributed to T_d-V^{5+} inside the walls and a band at 340 nm is assigned to T_d-V^{5+} on the wall surfaces of as-synthesized V-MCM-41 structure. Also, the other researchers have suggested that vanadium species can be incorporated both in the framework sites and in the wall surfaces [3,13,14].

Table 1

Assignment of UV–Vis DRS of V species in V-containing molecular sieves

Band (nm)	Assignment[a]	Reference
250	$V^{5+}(T_d)$ in the framework	[16,17]
340	$V^{5+}(T_d)$ in the surface	[9,16,17]
330–500	$V^{5+}(O_h)$	[19]
410	V^{5+}(sq. py.)	[17]
450	V^{5+}(distorted O_h)	[19]
605	$V^{4+}(T_d)$	[9,17,19]

[a] T_d: tetrahedral; O_h: octahedral; sq. py: square pyramidal.

After dehydration at 723 K in this study, all samples except V-MCM-41 show double bands at 220 and 250 nm and a shoulder at 350 nm. A band at 250 nm is associated with T_d-V^{5+} species. To elucidate the change of vanadium centers during hydration/dehydration, we have characterized the UV–Vis DRS change of all the four samples before and after contacting with air. Upon exposing the sample with air for 1 h, the absorption intensity in the region of 250 nm decreases, but the intensity of the 330 nm band increases except for V-MCM-41. This indicates that V^{5+} species are changed from tetrahedral into octahedral structure by contacting with the water molecules in the air. From Fig. 1, spectrum of V-MCM-41 is changed remarkably as compared to others. This represents that vanadium species of V-MCM-41 are incorporated much more than the other samples at the wall surface sites with no vanadium clusters, because the band at wavelength longer than 350 nm can be assigned to square pyramidal or octahedral V^{5+} on the wall surfaces. It is observed that the exposure causes color change from white to yellow and the spectral change is consistent with increasing coordination with water molecules to form square pyramidal and then octahedral geometries. From UV–Vis DRS data, it can be deduced that the most of the vanadium species are incorporated with tetrahedrally coordinated structure. In the case of V-MCM-41, water molecules have an easier access to vanadium species, indicating that most of the vanadium species exist in the wall surface of the MCM-41 channel. From FT-IR absorption at 960 cm^{-1} was observed, which is associated with the presence of vanadyl group (V=O) in the framework position of the molecular sieves.

All the vanadium-containing molecular sieves exhibit a pre-edge peak from the V K-edge XANES of Fig. 2. This can be assigned to the 1s–3d transition caused by the mixing of 2p orbitals of the oxygen anions with the 3p orbitals of the vanadium atoms [20], which suggest the presence of a tetrahedrally coordinated V^{5+} oxide species with a terminal vanadyl group in the molecular sieves.

The redox behavior of vanadium-containing samples was studied by electron paramagnetic resonance. In the case of as-synthesized samples, the EPR spectra do not have similarity with one another. The

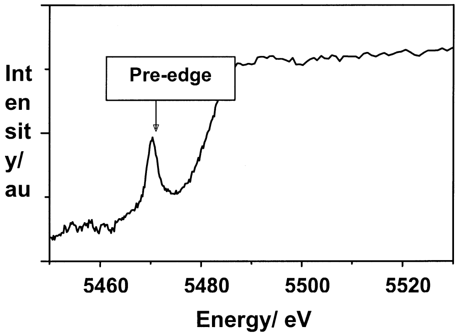

Fig. 2. XANES of V-MCM-41.

as-synthesized VS-1 sample exhibits only eight-line hyperfine spectra with two sets of Hamiltonian parameters, indicating the existence of at least two different V^{4+} environments. One is $g_{\parallel} = 1.9430$, $A_{\parallel} = 180\,G$ and $g_{\perp}=1.979$, $A_{\perp}=65\,G$ and the other is $g_{\parallel} = 1.939$, $A_{\parallel} = 191\,G$ and $g_{\perp}=1.984$, $A_{\perp}=63\,G$ corresponding to those of O_h-V^{4+} species [18]. However, the dehydrated VS-1 sample shows only one set parameter [$g_{\parallel} = 1.956$, $A_{\parallel} = 210\,G$ and $g_{\perp}=1.980$, $A_{\perp}=62\,G$] attributed to T_d-V^{4+}, while the calcined samples are EPR inactive due to the existence of V^{5+} only in the molecular sieves [19]. This indicates that, among two different environments in as-synthesized sample of VS-1, only one vanadium species have the redox property. EPR spectra of as-synthesized samples of V-MCM-41, V-MCM-48, and V-BEA show the single broad line without anisotropy (g=1.967) due to the presence of paramagnetic O_2^- radical, representing the existence of V^{4+} ions in a tetrahedral environment [21]. All of the calcined and dehydrated vanadium-containing molecular sieves give similar EPR signals at 77 K with anisotropy. The EPR signals of these materials indicate that V^{4+} species are located in square pyramidal coordination [9,16,17]. After calcining the as-synthesized samples in the air, all vanadium species are oxidized from V^{4+} to V^{5+} but some V^{5+} species can be reduced reversibly by dehydration at 723 K, indicating reversible redox properties. It seems that the vanadium species possessing redox property is responsible for the catalytic activities.

3.2. Catalytic activity test

Table 2
Hydroxylation of benzene over V-containing molecular sieves with H_2O_2 (reaction conditions: catalyst 0.05 g, benzene=acetic acid=6 ml, 30% H_2O_2=6.9 ml, 323 K, 6 h)

Catalyst	Si/V	TON (mol/mol-V)	Conversions[a] (%)
VS-1	33.3	3.8	0.046
VS-1[b]	33.3	13.3	0.16
VS-1[c]	33.3	27.3	0.33
V-BEA	60	9.5	0.19
V-MCM-41	55.7	24.3	0.53
V-MCM-41[d]	55.7	33.7	0.73
V-MCM-41[e]	55.7	64.4	1.39
V-MCM-41[f]	55.7	33.4	0.72
V-MCM-41[g]	55.7	2.4	0.053
V-MCM-48	100	36.2	0.44

[a] Selectivity higher than 93%.
[b] Catalyst: 0.1 g.
[c] Catalyst: 0.2 g.
[d] Temperature=333 K.
[e] Temperature=343 K.
[f] Temperature=353 K.
[g] No acetic acid added.

As shown in Table 2, mesoporous materials such as V-MCM-41 and V-MCM-48 show higher catalytic activity for benzene hydroxylation than microporous materials such as VS-1 and V-BEA. The conversion of benzene into phenol is in the range 0.04–1.39%. The higher activity of V-MCM-41 is thought to be due to the good dispersion of active sites, originating from vanadium species in the framework sites. The reason for the lowest catalytic activity over VS-1 seems to be that only a limited amount of vanadium ions have been incorporated into silicalite structure. When 0.2 g of VS-1 was used, the production of phenol is seven times higher than when 0.05 g of VS-1 was used. When the amount of acetic acid is increased, the conversion also is increased over V-MCM-41. The effect of reaction temperature is also compared, resulting that the higher temperature is favorable for obtaining the higher conversions. But the conversion at 353 K is lower than at 343 K because, probably, the decomposition of H_2O_2 have been accelerated during reaction at 353 K.

4. Conclusions

All vanadium-containing molecular sieves prepared in this study are active for hydroxylation of benzene. Vanadium species are able to incorporate into the framework sites as well as the surface of the wall, while both of them act as active sites for the hydroxylation of benzene. Based on the present reaction results, mesoporous materials such as V-MCM-41 and V-MCM-48 show higher catalytic activities than microporous materials such as VS-1 and V-BEA. There are two reasons why vanadium-containing mesoporous molecular sieves show higher activities for hydroxylation of benzene than microporous molecular sieves. One is that mesoporous molecular sieves make benzene molecule favorable to move easily towards active sites due to their large pore sizes. The other is that mesoporous molecular sieves have very high surface area where they provide active sites. In the case of microporous molecular sieves, benzene hydroxylation seems to have occurred rather on the surface than inside the channel because the kinetic diameter of benzene is 5.8 Å, while pore sizes are 5.4 and 6–7 Å for VS-1 and V-BEA, respectively. Also it can be thought that lower activity of microporous molecular sieves may be attributed to relatively lower number of silanol defect sites on the surface, where the vanadium ions can be anchored, in comparison with the mesoporous materials. According to UV–Vis DRS, V-MCM-41 has more surface vanadium species than the others which seems to be one of the reasons for higher catalytic activity as found in this work. It can be concluded that vanadium species on the surface wall as well as the framework provide active site even though we could not estimate which vanadium species between the surface wall and the framework sites.

References

[1] J.S. Beck, J.C. Vatuli, W.J. Roth, M.E. Leonowicz, C.T. Krege, K.D. Schmitt, T.-W. Chu, D.H. Olson, E.W. Sheppard, S.B. McCullin, J.B. Higgins, J.L. Schlenker, J. Am. Chem. Soc. 114 (1992) 10834.
[2] W.Z. Zhang, J. Wang, P.T. Tanev, T.J. Pinnavaia, J. Chem. Soc., Chem. Commun. (1996) 979.
[3] K.M. Reddy, I. Moudrakovski, A. Sayari, J. Chem. Soc., Chem. Commun. (1994) 1059.
[4] Z.Y. Yuan, S.Q. Liu, T.H. Chen, J.Z. Wang, H.X. Li, J. Chem. Soc., Chem. Commun. (1995) 973.
[5] D. Zhao, D. Goldfarb, J. Chem. Soc., Chem. Commun. (1995) 875.
[6] N. Ulagappan, C.N.R. Rao, J. Chem. Soc., Chem. Commun. (1996) 1047.
[7] B. Notari, Stud. Surf. Sci. Catal. 47 (1987) 413.
[8] T. Blasco, A. Corma, M.T. Navarro, J. Perez Pariente, J. Catal. 156 (1995) 65.
[9] T. Sen, V. Ramaswamy, S. Ganapathy, P.R. Rajamohanan, S. Sivasanker, J. Phys. Chem. 100 (1996) 3809.
[10] T. Tatsumi, K.Yuasa, H. Tominaga, J. Chem. Soc., Chem. Commun. (1992) 1446.
[11] T. Miyake, M. Hamada, Y. Sasaki, M. Oguri, Appl. Catal. 131 (1995) 33.
[12] S.-E. Park, J.W. Yoo, W.J. Lee, C.W. Lee, in: Proceedings of the 12th IZC, Baltimore, USA, Vol. II, 1999, 1253 pp.
[13] R. Schmidt, M. Stocker, D. Akporiaye, H.E. Torstad, A. Olsen, Microporous Mater. 5 (1995) 1.
[14] S.-H. Chien, J.-C. Ho, Mon Zeolites 18 (1997) 182.
[15] M.S. Rigutto, H. Van Bekkum, Appl. Catal. 68 (1991) L1.
[16] Z. Luan, J. Xu, H. He, J. Klinowski, L. Kevan, J. Phys. Chem. 100 (1996) 19595.
[17] K.J. Chao, C.N. Wu, H. Chang, L.J. Lee, Shu-fen, Hu, J. Phys. Chem. B 101 (1997) 6341.
[18] G. Centi, S. Perathoner, F. Trifiro, A. Aboukais, C.F. Aissi, M. Guelton, J. Phys. Chem. 96 (1992) 2617.
[19] J. Kornatowski, B. Wichterlova, J. Jirkovsky, E. Loffler, W. Pilz, J. Chem. Soc., Faraday Trans. 92 (1996) 1067.
[20] S.G. Zhang, S. Higashimoto, H. Yamashita, M. Anpo, J. Phys. Chem. B. 102 (1998) 5590.
[21] V.A. Shvets, V.B. Kazansky, J. Catal. 25 (1972) 123.